International Journal of Geo-Engineering

RESEARCH Open Access

Cement-stabilized marine clay under thermal cycling: strength, suction, and microstructure

Zhe Liu[1] and Mamadou Fall[1*]

*Correspondence:
Mamadou Fall
mfall@uottawa.ca
[1]Department of Civil Engineering, University of Ottawa, 161 Colonel By, Ottawa, ON K1N 6N5, Canada

Abstract

This study investigates the influence of realistic summer daily thermal cycles on the mechanical, hydraulic, and microstructural properties of cement-stabilized sensitive marine clay (SMC), a problematic marine soil widely found in Eastern Canada. SMC samples treated with 5% and 20% cement were subjected to two curing regimes: constant temperature (20 °C) and simulated daily thermal cycles, and tested after 1, 3, 7, and 28 days of curing. Unconfined compressive strength (UCS) and secant modulus tests were performed to assess mechanical performance, while matric suction monitoring, thermogravimetric analysis (TG/DTG), and mercury intrusion porosimetry (MIP) were used to evaluate hydration behavior and microstructural evolution. Results show that daily thermal cycles significantly accelerate strength and stiffness development at early curing stages by enhancing cement hydration, leading to finer pore structures and higher matric suction due to rapid self-desiccation. However, a "crossover effect" was observed in TG/DTG results, where prolonged thermal cycling reduced hydration product formation at later stages. MIP results, in contrast, showed continued microstructural densification, likely due to a dilution effect associated with high water-to-cement ratios. These findings provide practical insights for optimizing curing strategies and binder dosages in road and infrastructure projects involving sensitive marine clays under fluctuating thermal conditions.

Keywords Daily thermal cycles, Cement stabilization, Sensitive marine clay, Hydration, Microstructure, Matric suction, Mechanical properties

Introduction

Sensitive marine clays (SMCs), such as those found in Eastern Canada—particularly in Quebec, Ontario, and the Maritime provinces—are problematic soils known for their high sensitivity and tendency to lose significant strength upon disturbance. These clays, typically formed in glaciomarine or post-glacial marine environments, also occur in other parts of the world, including Scandinavia, Japan, Russia, Chile, Alaska, northern China, and New Zealand [32, 42]. In Canada, large urban areas such as Ottawa, Montreal, and Quebec City are underlain by SMC deposits, commonly referred to as Leda clay [2, 11, 56, 57]. These clays often form the subgrade for road infrastructure, which plays a fundamental role in supporting pavement systems [65]. However, due to their

low shear strength, high compressibility, and sensitivity, untreated SMCs are unsuitable for direct use in pavement subgrades. In regions such as Ottawa, SMC deposits can reach depths of 600 feet and thicknesses of up to 200 feet [16], necessitating the use of stabilization techniques to enhance their engineering properties.

Cement stabilization is one of the most widely used methods to improve the strength, stiffness, and durability of SMCs [33]. The primary mechanism involves the hydration of cement, leading to the formation of cementitious products such as calcium silicate hydrate (C–S–H), ettringite, and portlandite (CH), which bind clay particles and refine the pore structure [19, 52]. Several researchers have explored the effectiveness of various binders, including lime, fly ash, and ground granulated blast furnace slag (GGBFS), in stabilizing problematic soils [67]. For instance, lime has been shown to improve strength significantly through pozzolanic reactions [61], while fly ash and GGBFS have been used to enhance long-term performance [3, 34].

In particular, slag-based composite binders and supplementary cementitious materials have attracted increasing attention due to their improved sustainability, lower carbon footprint, and potential economic advantages compared to ordinary Portland cement. These alternative binders have demonstrated promising long-term strength development and durability in stabilized soils.

Nevertheless, cement remains the most widely adopted stabilizer in road and infrastructure projects due to its rapid reactivity, predictable performance, and widespread availability, particularly for large-scale infrastructure applications [4, 49]. In practical pavement construction, cement is often preferred as an industry-standard binder because it provides reliable early-age strength gain, which is critical for construction scheduling and early traffic loading. Moreover, cement serves as a baseline reference material for understanding stabilization mechanisms, against which the performance of alternative binders can be meaningfully compared. Therefore, cement was selected in this study as a representative and practical stabilizer to establish fundamental understanding of thermal cycling effects on stabilized sensitive marine clays.

The strength development of cement-stabilized soils is influenced not only by binder content but also by curing conditions, especially temperature [39]. Elevated temperatures accelerate the rate of cement hydration, leading to rapid early strength gains [37]. However, prolonged curing at high temperatures may lead to the formation of dense hydration product layers that hinder further hydration—a phenomenon known as the "crossover effect" [14, 40]. This effect has been explained by the Protective Layer Theory, which suggests that the rapid precipitation of hydration products around unhydrated cement particles impedes continued reaction [31, 55].

Most prior studies investigating the influence of curing temperature on cement-stabilized soils have employed constant temperature regimes, which may not reflect the fluctuating conditions experienced in real field environments. In practice, subgrades are subjected to diurnal temperature variations, especially during summer months when soil surface temperatures can exceed air temperatures due to solar radiation [62]. These daily thermal cycles could affect hydration kinetics, pore water distribution, self-desiccation, and ultimately the mechanical performance of stabilized subgrades. Yet, the effects of realistic summer daily thermal cycles on the behavior of cement-stabilized SMC have not been thoroughly explored, representing a critical knowledge gap.

Therefore, the objective of this study is to experimentally investigate the influence of daily summer thermal cycles on the strength development, stiffness evolution, matric suction, and microstructural changes of cement-treated sensitive marine clay. Understanding these effects is vital for optimizing binder usage and curing practices, and for developing durable and cost-effective pavement systems on thermally affected subgrades.

Materials and experimental program

Materials

Sensitive marine clay

This study focuses on SMC from Eastern Canada, also known as Leda or Champlain Sea clay, which was collected from the Canadian Geotechnical Research Site in Gloucester, Ottawa, Ontario, at a depth of 3 m below the ground surface. The main constituents of this clay are identified as quartz, feldspars, illite, chlorite, along with amorphous materials. Mineralogical analyses indicate that clay minerals (primarily illite and chlorite) account for approximately 87% of the total mineral composition of the soil. Carbonate minerals, such as calcite and dolomite, accounts for about 1–2% of the total weight of the clay [8, 43, 47]. In contrast, grain size distribution analysis based on sieve and hydrometer methods (Fig. 1) shows that the clay-size fraction (< 2 μm) represents approximately 12% of the total soil mass, with the remainder consisting of silt- and sand-sized particles. Furthermore, key index properties of the clay were determined according to ASTM standards, and the results are summarized in Table 1.

Cement and mixing water

In this study, Portland cement Ⅰ (PCI) was utilized as the sole binder, and its composition is presented in Table 2. For the mixing process, tap water was employed, maintaining a water-to-cement ratio of 1:1. Two different binder content levels, specifically 5% and 20%, were selected. The selected binder dosages were chosen to represent two practical stabilization levels commonly encountered in soil improvement applications.

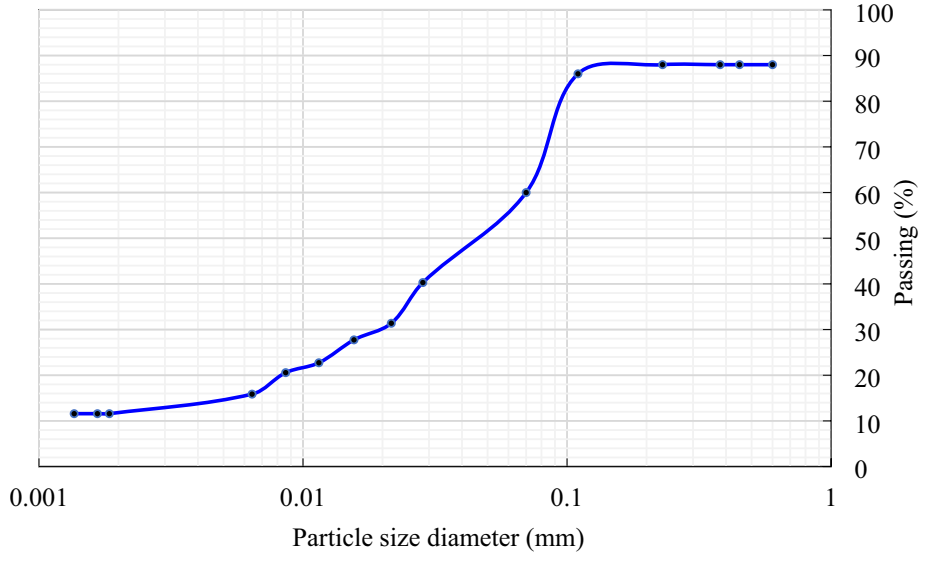

Fig. 1 Grain size distribution of SMC

Table 1 Properties of SMC

Properties	Value/classification	ASTM standards
Unified soil classification system	CH	
Natural moisture content (%)	53.6	ASTM D2216
Liquid limit, LL (%)	48	ASTM D4318
Plastic limit, PL (%)	21.5	ASTM D4318
Plastic index, PI (%)	26.5	ASTM D4318
Liquidity index, LI (%)	1.2	
Clay fraction (%)	87	
Activity	0.3	
Optimum water content, OMC (%)	26	ASTM D698
Maximum dry unit weight (g/cm^3)	1.5	ASTM D698
Specific gravity	2.67	ASTM D 854

Table 2 Main chemical and physical characteristic PCI

Element	SO_3	Fe_2O_3	Al_2O_3	SiO_2	CaO	MgO	Relative density
PCI (%)	3.82	2.70	4.53	18.03	62.82	2.65	3.2

Table 3 Mix proportions of cement-treated SMC samples

Sample	Dry SMC (g)	PCI (g)	Water (g)	W/C ratio
SMC5%	**1000**	**50**	**50**	**1:1**
SMC20%	**1000**	**200**	**200**	**1:1**

PCI mass corresponds to 5% and 20% of the dry SMC mass, respectively. Mixing water was added at a constant water-to-cement ratio of 1:1 following FHWA recommendations

The lower dosage of 5% corresponds to a minimal stabilization range aimed at achieving basic strength enhancement and workability improvement, while the higher dosage of 20% represents a high-strength stabilization level typically adopted when substantial strength and stiffness gains are required. Together, these two levels define practical lower and upper bounds of cement content in field stabilization, allowing assessment of daily thermal cycling effects across a wide performance range.

Sample preparation and curing

Sample preparation

In this study, the wet mixing method was employed. This approach is widely used in both laboratory studies and field deep mixing applications for soft and high-moisture marine clays, where slurry-based binder injection and intensive mixing are commonly adopted to achieve uniform stabilization. Dry mixing is also common but is only applicable to soils with a natural moisture content exceeding 60% [12]. The sample preparation followed the Federal Highway Administration Manual [12], which recommends wet mixing procedures for soft cohesive soils to ensure effective binder dispersion and homogeneity. First, the required amount of SMC was determined. Binder content was defined as the mass percentage of Portland cement I (PCI) relative to the dry mass of SMC, and two levels of binder content (5% and 20%) were adopted in this study. Since the binder consisted entirely of PCI, the PCI content was 100% for all mixtures. The corresponding masses of SMC, PCI, and mixing water for each mixture are summarized in Table 3. The clay was then placed in a mixer for 3 min to blend and ensure the homogeneity. The mixer bowl was covered to prevent evaporation during blending. Subsequently, the required amounts of PCI and water were determined, and the mixture was blended in

another mixer for 3 min, maintaining a water-cement ratio of 1:1 [12]. This water-to-cement ratio was selected to account for the high natural moisture content of sensitive marine clay and to produce a workable cement slurry that facilitates uniform mixing and effective binder dispersion within the soil matrix. Such slurry consistency is commonly adopted in field deep mixing and soft ground stabilization practices to ensure homogeneity and reliable strength development. The cement slurry was then slowly added along the inner walls of the mixing bowl while the mixer was running. The mixture of SMC, PCI and water was mixed for another 9 min. This wet mixing process replicates field slurry mixing techniques used in soft ground improvement and deep soil stabilization projects, thereby enhancing the practical relevance of the laboratory procedure. Following mixing, the prepared mixture was placed into cylindrical molds with a diameter of 50 mm and height of 100 mm. Each mold was filled in three layers, and external vibration was applied to remove air bubbles and ensure uniformity. The filling process was completed within 30 min to avoid discrepancies in moisture content due to evaporation. The samples prepared were sealed to prevent moisture loss and cured under two different temperature conditions: a constant temperature of 20 °C and daily thermal cycles, as summarized in Table 4. Samples were cured for 1, 3, 7, and 28 days prior to testing.

Sample curing

In this study, the cement-stabilized SMC samples were subjected to different thermal curing conditions to investigate their effects on the mechanical and physical properties. The curing process is crucial as it significantly influences the hydration of cement and, consequently, the performance of the treated SMC. Two modes of thermal curing were employed for the prepared samples:

(i) Constant laboratory temperature (control samples): One group of samples was cured under a constant laboratory temperature of 20 °C. These samples served as the reference control group for comparing with the sample group cured under daily thermal cycle conditions.

(ii) Daily thermal cycle (simulating field conditions in Ontario, Canada): Another group of samples was subjected to curing conditions with temperature fluctuations to investigate the effect of daily thermal cycles on the performance of cement-stabilized SMC. The samples in this study were cured under simulated summer daily thermal cycles. The highest recorded temperature in Ontario, 42.2 °C, occurred in 1936 [15, 21]. In field conditions, soil surface temperature is typically higher than air temperature due to solar radiation. Continuous exposure to intense sunlight during summer significantly elevates surface temperature [7]. The peak daily soil

Table 4 Summary of curing condition of samples

Sample nomenclature	Binder content* (%)	Curing times (days)	PCI content (%)	Curing temperature (°C)
SMC5%-20 °C	5	1, 3, 7 and 28	100	20
SMC5%-Daily Thermal Cycle	5	1, 3, 7 and 28	100	Daily thermal cycles
SMC20%-20 °C	20	1, 3, 7 and 28	100	20
SMC20%-daily thermal cycle	20	1, 3, 7 and 28	100	Daily thermal cycles

* Binder content is defined as the mass percentage of PCI relative to the dry mass of sensitive marine clay (SMC). Since the binder consists entirely of PCI, the PCI content is 100% for all mixtures

temperature is determined by the models which consider the factors including air temperature and solar radiation [5, 53].

Figure 2(a) presents the maximum daily temperature applied to the samples during the 28-day curing period. Cement hydration progresses rapidly in the initial stages, and the hydration reaction is highly sensitive to temperature during this period [38, 41]. Therefore, the highest curing temperatures were arranged within the first few days of curing. Figure 2(b) illustrates the application of daily thermal cycles throughout the 28-day curing period. It is worth noting that only the highest temperatures are shown in the figure, as these are of particular interest. Additionally, the thermal cycles extended beyond the three cycles depicted in the figure.

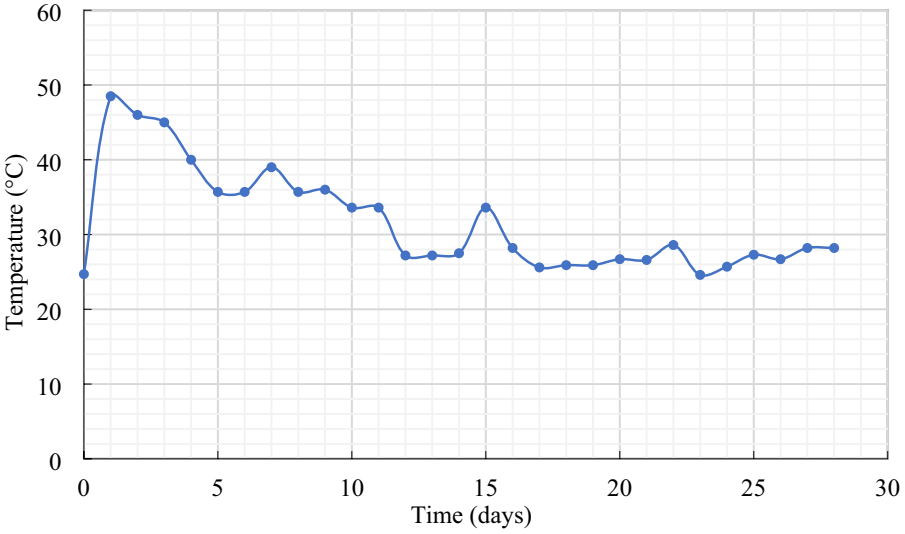

(a) Maximum daily temperatures applied to samples

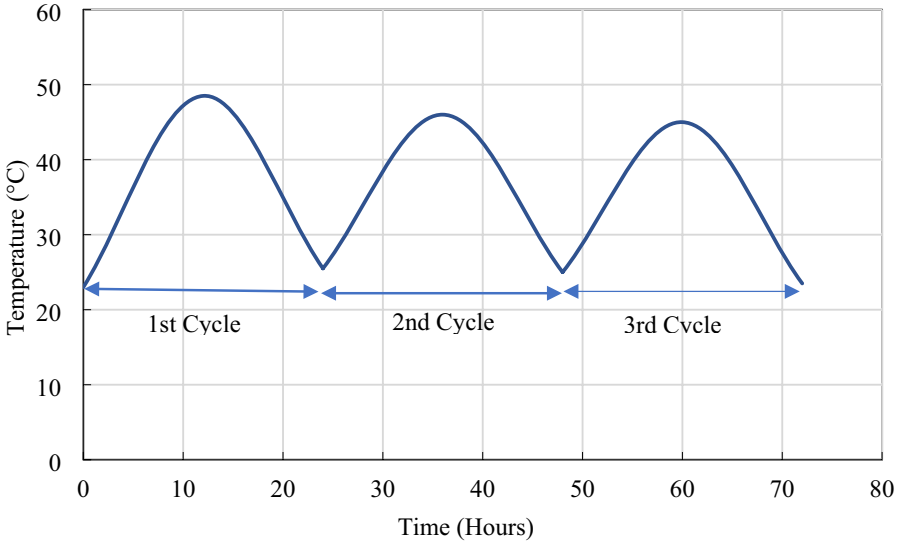

(b) Thermal cycles with maximum temperatures applied to samples

Fig. 2 Maximum daily temperatures and thermal cycles to be applied to samples

After preparation, the samples were sealed and placed in an oven for curing. Temperature regulation during curing was conducted by an Inkbird ITC-608T temperature controller, with a control range of -40 °C to 100 °C and a precision of 0.1 °C. During the curing process, temperature increases and decreases were adjusted stepwise in a gradient manner. Each daily thermal cycle was divided into six stages to simulate realistic fluctuations.

Testing and monitoring method

Mechanical test

The UCS test was conducted on cement-stabilized SMC samples after curing for 1, 3, 7, and 28 days, in accordance with the guidelines of ASTM C39/C39M-21. The test was performed using the ELE Digital Tritest 50 Load Frame, with a loading rate set to 1 mm/min. The load frame has a maximum capacity of 50 kN. Throughout the UCS tests, pictures of the samples were taken to observe and compare different failure modes. All test data was collected via an internal linear variable differential transformer connected to an electronic data acquisition system. The secant modulus was determined from the recorded stress–strain curves as the slope of the line connecting the origin and the point corresponding to 50% of the peak UCS value, providing a representative measure of sample stiffness during loading.

Monitoring program

Matric suction monitoring experiments were conducted to investigate the suction of cement-stabilized SMC samples with varying cement content and curing conditions. The monitoring was carried out using the ECH2-MPS-6 dielectric water potential sensor, which has a measurement range from − 9 kPa to -100,000 kPa and an accuracy of ± (10% of reading + 2 kPa) within the range of -9 kPa to -100 kPa. Prior to testing, the sensors were calibrated following the manufacturer's recommended procedures and verified under controlled moisture conditions to ensure reliable measurements. To ensure accurate measurements, molds with larger dimensions (100 mm in diameter × 200 mm in height) were used, providing ample space for sensor. The sensors were carefully embedded at the center of the specimens to minimize boundary effects, and the molds were properly sealed to prevent moisture loss during curing and monitoring. Data was collected by an EM50 data logger, and matric suction was monitored over a 28-day curing period.

Microstructural analysis

MIP test was employed to analyze the pore structure of cement-stabilized SMC samples. The test was conducted using the Micromeritics AutoPore IV 9500 Series porosimeter. In this analysis, mercury was intruded into the samples at various pressure levels because the pressure required for intrusion is inversely proportional to the pore size. The samples were dried in an oven at 45 °C for 4 days as a low-temperature drying procedure commonly adopted to minimize microstructural disturbance in soil–cement materials compared to higher oven-drying temperatures. This approach was selected to reduce the risk of shrinkage and microcracking while still ensuring sufficient moisture removal prior to mercury intrusion. The samples were then cut into 10 mm × 10 mm × 5 mm cubes for MIP test.

Thermogravimetric analysis and derivative thermogravimetry (TG/DTG) test was conducted on cement paste samples cured under the same conditions as the cement-stabilized SMC samples to evaluate the cement hydration level. Cement paste was selected instead of cement-treated SMC to isolate the hydration behavior of the binder, since direct TG/DTG analysis on stabilized clay is strongly influenced by the thermal decomposition of clay minerals, carbonates, and bound water within the soil matrix, which can overlap with cement hydration signals and obscure the interpretation of hydration products. The cement paste samples were placed in an oven at 45 °C for 4 days until their weight stabilized, before being ground into a fine powder and sieved through a No. 200 mesh sieve. The TG/DTG measurements were performed using a Q5000 TG analyzer which monitored weight loss as the furnace temperature was gradually increased up to 1000 °C at a heating rate of 10 °C/min. These analyses provided insights into the hydration characteristics of the cement paste under the given curing conditions.

Results and disscussion

Effect of daily thermal cycles on strength and modulus development

The effects of daily thermal cycles on the development of the UCS of SMC samples with 5% and 20% cement content are illustrated in Fig. 3. The four strength development curves in Fig. 3 demonstrate a general increasing trend throughout the 28 day curing period, regardless of cement content (5% or 20%) and curing temperature (20 °C or daily thermal cycles). This reflects the progressive hydration of cement, which generates hydration products, such as C-S-H, CH and ettringite, that enhance the cohesion by bonding soil aggregates and filling capillary pores [26, 28, 36, 59, 64]. Moreover, under the same curing time, the samples with 20% cement content exhibit higher strength than the ones with 5% cement content. This is because a higher cement content leads to more cement participating in the hydration reaction, generating a greater amount of hydration products. These products form more effective bonds between the clay particles and fill more pores within the samples, leading to a denser structure and, consequently, improved the strength [3].

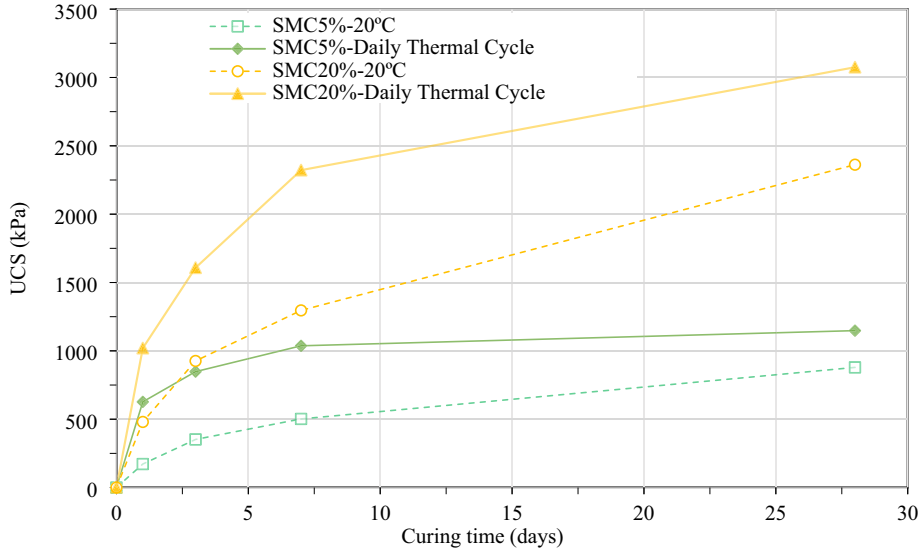

Fig. 3 Development of the UCS of SMC samples with 5% and 20% cement content

As shown in Fig. 3, the strength of samples with cement content of 5% and 20% cured under daily thermal cycle conditions is higher than that of samples cured at room temperature. This strength difference is most pronounced on the first day of curing. For instance, the 1-day strength of the SMC20%-Daily Thermal Cycle samples is 1020 kPa, which represents a 113% increase compared to the control group (480 kPa). Similarly, the 1-day strength of the SMC5%-Daily Thermal Cycle samples is 627 kPa, showing a 265% increase compared to the control group (172 kPa). This strength difference gradually diminishes over the curing period. After 28 days, the strength of the samples with cement content of 20% and 5%, cured under daily thermal cycle conditions, is 30% and 31% higher, respectively, compared to those cured at 20 °C. The observed strength enhancement can be attributed to the promotion of the hydration reaction by the high temperature [13]. In this scenario, hydration products are rapidly formed, filling the capillary pores of the samples and effectively reducing their porosity [6, 10, 17, 22, 25, 29, 45, 46, 54]. Moreover, strong bonds are quickly formed between the clay particles within a relatively short period, creating an interlocking structure that significantly enhanced the strength of the samples [66]. Moreover, the UCS increase rate follows a general trend of gradual decline as curing progresses, regardless of cement content and curing temperature conditions. This can be attributed to the consumption of reactants as the hydration reaction proceeds, leading to a gradual slowdown in the reaction rate and a corresponding reduction in the rate of strength increase [23]. However, the rate of strength development varies significantly under different curing temperature conditions, as shown in Fig. 4. It can be observed that from day 1 to day 7, the strength development rate of the samples cured under daily thermal cycling is higher than that of the control group cured at 20 °C. This difference is most pronounced from day 1 to day 3. However, from day 7 to day 28, the strength development rate of the samples cured under daily thermal cycling is significantly lower than that of the samples cured at 20 °C. Under the curing conditions of daily thermal cycles, the strength of the samples increases significantly in the early curing stage, reaching a relatively high level within the first seven days. This has important implications for shortening construction period and controlling costs.

The failure modes of SMC samples cured for 28 days under different conditions are depicted in Fig. 5. The observed failure patterns reveal the significant influence of

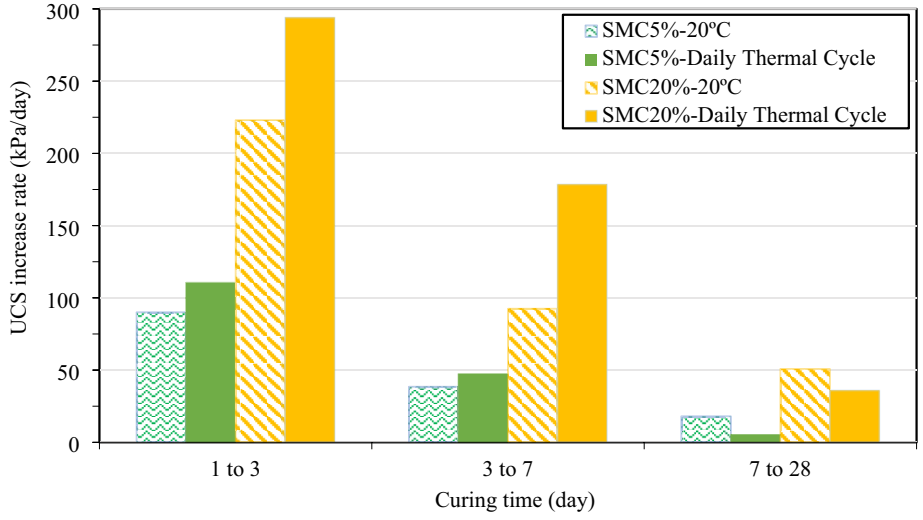

Fig. 4 Average increase in strength at different time interval

curing temperature on the mechanical behavior of the samples. Samples cured under daily thermal cycles exhibit more prominent and widely distributed cracks compared to those cured at a constant temperature of 20 °C. Failure in the samples cured under daily thermal cycles occurred more rapidly. The SMC20%-Daily Thermal Cycle samples demonstrated a sudden failure accompanied by an audible brittle fracture. This behavior indicates that higher curing temperature leads to stiffer samples with reduced plastic deformation, resulting in a predominantly brittle failure mode, especially in samples with higher cement content. In contrast, samples cured at a constant temperature of 20 °C display a classic ductile failure mode, characterized by a prolonged plastic deformation before failure.

Figure 6 shows the effects of daily thermal cycles on the development of the secant modulus of SMC samples with 5% and 20% cement content. During the 28-day curing period, the development of the secant modulus follows a pattern similar to that of strength. The secant modulus increases with curing time, but the rate of increase slows down over time, which is independent of curing temperature and cement content. Under the daily thermal cycles, the secant modulus of the samples is higher than that of

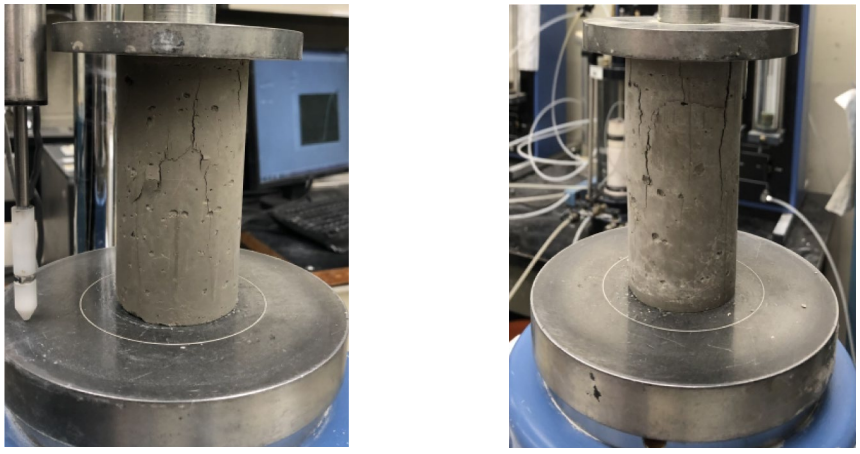

(a) SMC5%-20°C (b) SMC5%-Daily Thermal Cycle

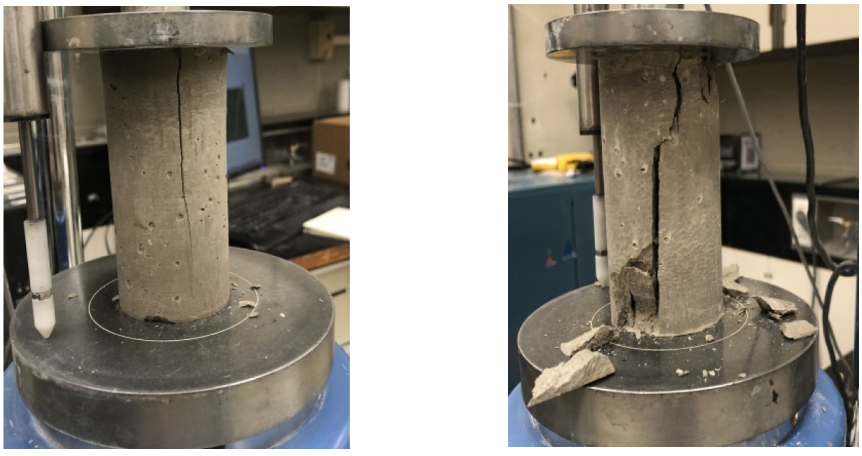

(c) SMC20%-20°C (d) SMC20%-Daily Thermal Cycle

Fig. 5 Failure modes of samples cured for 28 days

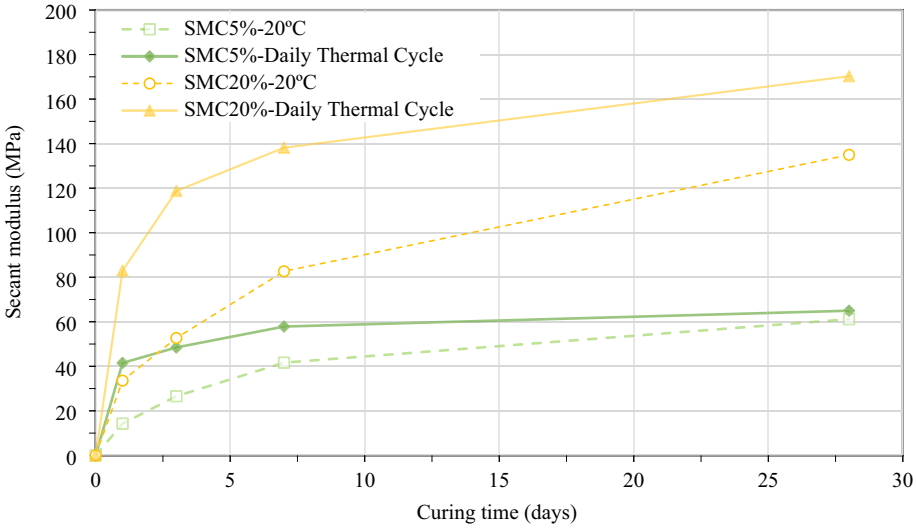

Fig. 6 Secant modulus change with curing time

samples cured at 20 °C. This is similar to the effect of daily thermal cycles on the strength of the samples and can be explained by the promotion of cement hydration due to higher curing temperatures. Additionally, a higher cement content significantly enhances stiffness, as evidenced by the substantially higher secant modulus values in samples with 20% cement content. The mechanisms behind this increase in modulus are similar to those responsible for the increase in UCS of the samples with higher cement content, as described earlier. However, the effect of daily thermal cycles on stiffness development appears to be more significant. For samples with 20% cement content, the 3-day stiffness reaches 70% of the 28-day value under daily thermal cycle curing conditions, while for samples with 5% cement content, the 3-day stiffness reaches 75% of its 28-day stiffness. In comparison, at 20 °C, the 3-day stiffness for samples with 20% and 5% cement content is only 39% and 43% of their respective 28-day values. The secant modulus, which quantifies the stiffness of a material, reflects its capacity to resist deformation under applied stress. A higher secant modulus indicates a more rigid and stable structure, which is critical for the subgrade subjected to long-term loads [24]. For samples cured under daily thermal cycle conditions, a relatively high stiffness is achieved by the third day of curing. This indicates that daily thermal cycles enable the samples to quickly attain a higher resistance to deformation. This allows the subgrade to meet construction requirements more quickly, which is crucial for shortening the construction period.

These mechanical trends indicate that daily thermal cycles accelerate early hydration and promote faster formation of C-S-H, CH and ettringite, which densify the cement-treated clay fabric by filling capillary pores [28, 66]. This early densification is expected to increase capillary effects and self-desiccation, thereby increasing matric suction [18] and contributing to the higher early-age UCS and stiffness, which is further examined in the following suction and microstructural analyses.

Effect of daily thermal cycles on the matric suction

The results of matric suction monitoring are presented in Fig. 7. Generally, for all sample groups, matric suction increases with curing time, regardless of cement content and curing temperature. This increase is attributed to the cement hydration process, during

which the water within the samples is consumed continuously [18]. In addition, during the hydration process, hydration products such as C-S-H, CH and ettringite precipitate within the voids, which results in a finer structure. As the pore size decreases, capillary action is enhanced, which contributes to the development of negative pore pressure [44]. The higher suction observed in samples with 20% cement content compared to those with 5% cement content can be explained by the more intensive hydration reactions, which consume more water. More intensive water consumption in these samples causes a significant increase in pore water pressure, thereby resulting in higher matric suction [60].

The matric suction of samples cured under daily thermal cycles is significantly higher than that of samples cured at 20 °C with the same cement content. This difference is most evident during the early stage of curing. For the 3-day samples with 20% cement content, the matric suction under daily thermal cycles and 20 °C conditions are 460 kPa and 270 kPa, respectively. For the 3-day samples with 5% cement content, the matric suction values under the two conditions are 178 kPa and 48 kPa, respectively. This difference in matric suction is attributed to the rapid self-desiccation of the samples or cement hydration due to high curing temperature. Under high curing temperature during the early stage, the self-desiccation in the samples occurs more intensively and rapidly, resulting in a faster and more significant consumption of pore water [63]. Figure 8(a), the TG/DTG test results of the 3-day cement paste sample also clearly demonstrate that daily thermal cycles promote hydration and increase the consumption of capillary pore water in the early-stage. It can also be seen from Fig. 7 that the difference in matric suction of the samples cured under the two different thermal conditions gradually decreases with curing time. In other words, the influence of daily thermal cycles on the matric suction of the samples declines over time. On day 28, for the samples with 20% cement content, the matric suction under daily thermal cycles and 20 °C curing conditions are 725 kPa and 690 kPa, respectively. For the samples with 5% cement content, the values are 578 kPa and 518 kPa, respectively. It can be observed that on day 28, the matric suction of samples with the same cement content shows slight difference under the two different curing temperature conditions. As discussed earlier, during the early stage of curing, daily thermal cycles significantly accelerate the self-desiccation of the samples, leading

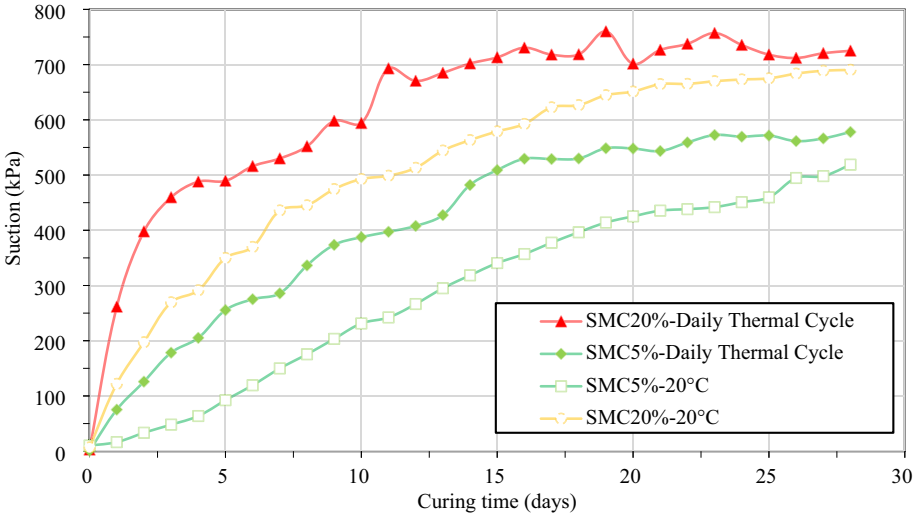

Fig. 7 The development of matric suction of cement-treated SMC

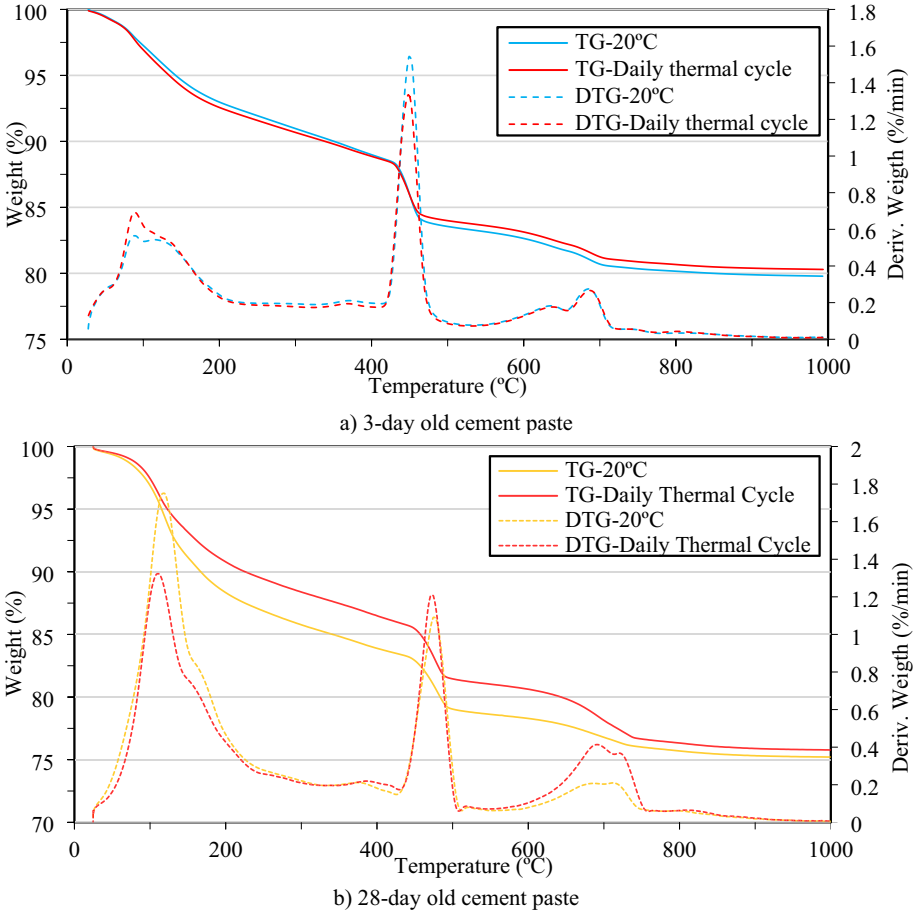

Fig. 8 TG/DTG analyses of cemented paste samples cured at 20 °C and daily thermal cycles

to the rapid consumption of water and a large amount of hydration reactants. According to hydration reaction kinetics, as the degree of hydration increases, the content of reactants decreases, the apparent activation energy of the reactants gradually decreases, and the hydration reaction gradually slows down [30, 58]. During the late stage, the samples cured under daily thermal cycle conditions have a lower cement content. Therefore, for the samples cured under daily thermal cycles, the apparent activation energy of the reactants is lower, resulting in a slower progression of self-desiccation and slower consumption of pore water, compared to the samples cured at 20 °C. Thus, the difference in matric suction of the samples cured at two different thermal conditions significantly decreases in the later stage of curing.

The findings about the impact of daily thermal cycles on the self-desiccation of cement-stabilized SMC may have significant engineering implications. The stability and safety of subgrade are among the most important factors in pavement design and construction. Moreover, the rapid development of subgrade strength helps shorten the construction period and control costs. The strength, safety, and opening time of the subgrade are significantly influenced by pore pressure. Daily thermal cycles accelerate the self-desiccation process of cement-stabilized SMC samples. This leads to a faster increase in suction and a more rapid increase in strength, ultimately resulting in an earlier subgrade activation time.

The suction evolution provides a hydro-mechanical explanation for the strength trends in Sect. "Effect of Daily Thermal Cycles on Strength and ModulusDevelopment". Accelerated hydration under daily thermal cycles increased water consumption and promoted pore refinement, which enhanced capillary action and led to higher matric suction [18, 44]. The higher suction levels, especially at early ages and higher cement contents, indicate stronger self-desiccation and a denser pore network [60], which is consistent with the higher UCS and secant modulus observed. These mechanisms are further supported by the TG/DTG and MIP microstructural results presented in the next section.

Effect of daily thermal cycles on microstructure

The results of the microstructural analyses are presented in Figs. 8, 9 and 10. The thermal analysis (TG/DTG) results of cement paste samples cured under different conditions and durations are shown in Fig. 8. The DTG curve represents the rate of change of TG values with temperature, with significant fluctuations or peaks corresponding to rapid weight loss in the TG curve. The weight loss observed between 25 °C and 100 °C primarily results from the evaporation of free or bound water [51]. In the 100 °C to 200 °C range, weight loss is attributed to the dehydration of hydrated products such as

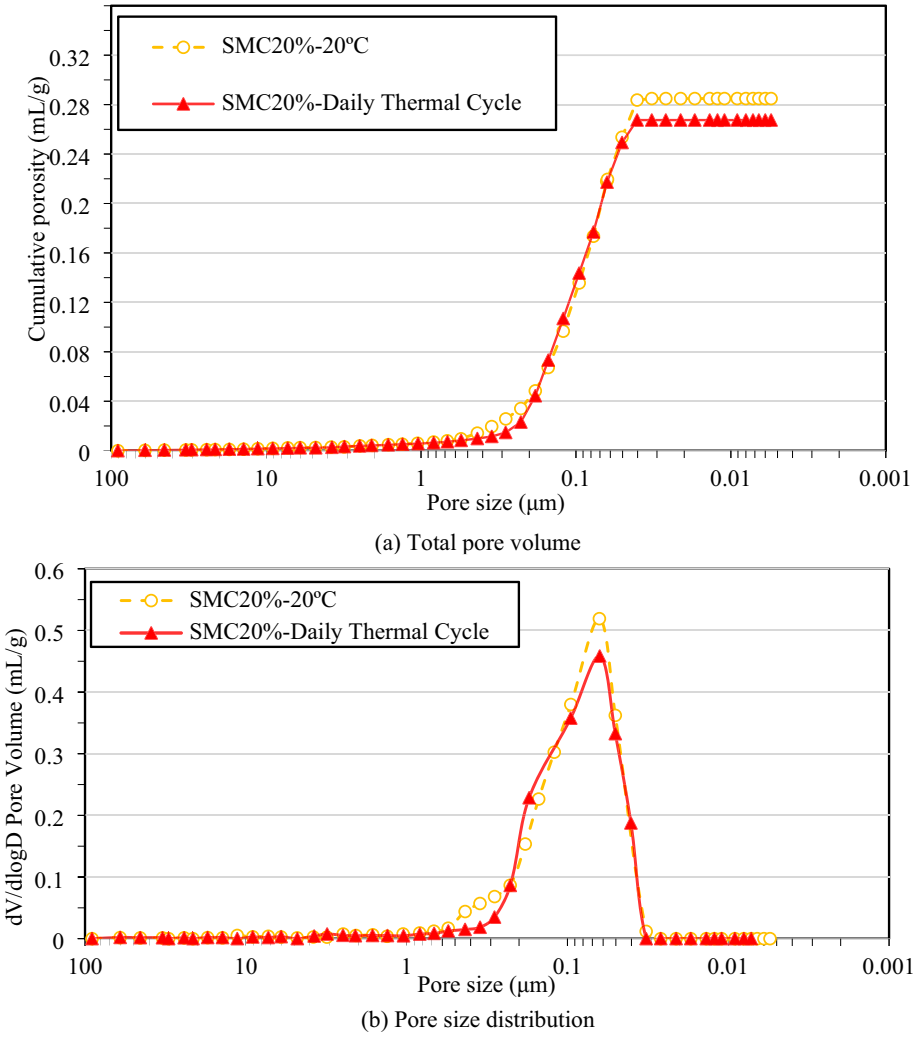

Fig. 9 MIP test results for 3-day samples curing at 20 ℃ and daily thermal cycles

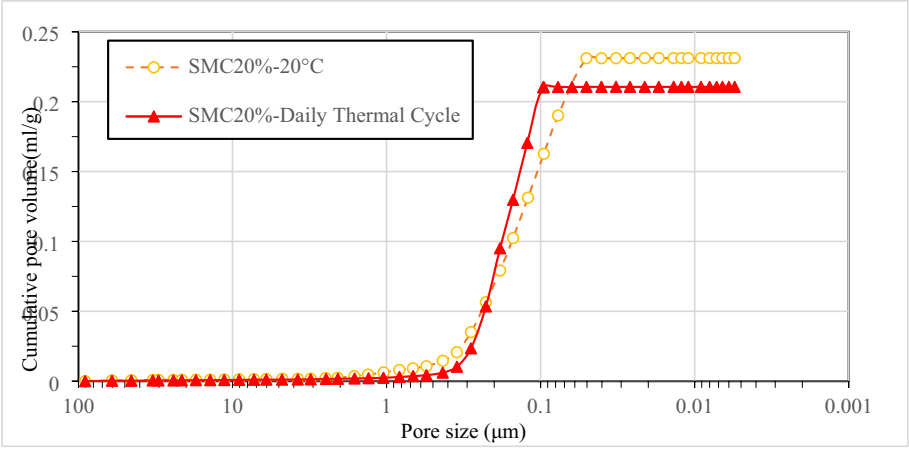

(a) Total pore volume

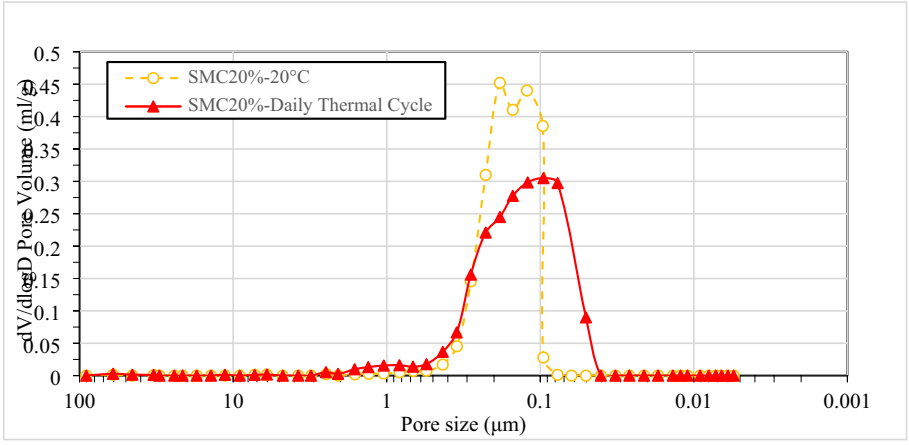

(b) Pore distribution

Fig. 10 MIP test results for 3-day samples curing at 20 °C and daily thermal cycles

C-S-H, gypsum, ettringite, and carboaluminates. For example, CSH undergoes dehydration, ettringite decomposes via a heterogeneous mechanism, carboaluminates experience partial dehydration and water loss, and gypsum decomposes through a double endothermic reaction [1]. The second major peak, observed between 425 °C and 525 °C, corresponds to the dihydroxylation of portlandite. The third peak, occurring between 650 °C and 900 °C, is attributed to the decarbonation of calcium carbonate [35, 50]. It should be noted that although specimens were carefully handled and dried at low temperature prior to testing, minor carbonation during storage or drying cannot be completely excluded. Such carbonation may contribute to the mass loss observed in this temperature range; however, its influence is expected to be limited and does not alter the comparative trends between curing conditions.

In Fig. 8(a), the 3-day cement paste sample subjected to daily thermal cycles exhibits a greater mass loss and a more pronounced peak in the 75–200 °C temperature range compared to the sample cured at a constant 20 °C. This slightly higher weight loss and intensified peak suggest that a greater quantity of hydration products—such as calcium silicate hydrate (C–S–H) and ettringite—were formed during the early stages of hydration, likely due to elevated temperatures accelerating the hydration reaction [55]. In

Table 5 Estimated portlandite (CH) content from DTG peak integration (425–525 °C)

Curing condition	$\Delta m_{425-525}$ (wt% H_2O of dry sample)*	CH content (wt% of dry sample)
20 °C curing	2.30	9.47
Daily thermal cycles	1.90	7.82

*$\Delta m_{425-525}$ was obtained by graphical digitization of TG curves over the temperature range 425–525 °C, corresponding to portlandite dehydroxylation. Values represent approximate estimates due to digitization from plotted curves; the same extraction procedure was applied to both curing conditions to ensure consistent comparison

contrast, the more prominent peak observed in the control sample within the 400–500 °C range is attributed to a higher content of calcium hydroxide (CH). This is consistent with the understanding that CH, also known as portlandite, can be consumed through pozzolanic reactions in clay soils, particularly when the soil contains reactive silica (SiO_2) and/or alumina (Al_2O_3)—both commonly found in sensitive marine clays (e.g., Boardman et al. [9], Khemissa, [27]. The quantitative CH estimates in Table 5 further confirm that samples cured under daily thermal cycles exhibit lower portlandite content, supporting enhanced CH consumption through pozzolanic reactions.

In contrast, Fig. 8(b) shows that after 28 days, the total weight loss is 24.2% for the sample cured under daily thermal cycles, compared to 24.8% for the sample cured at 20 °C, with the latter also exhibiting a more pronounced peak in the 75–200 °C temperature range. This indicates that the sample cured at 20 °C developed more hydration products over the 28-day period. The first peak, observed around 130 °C and associated with the decomposition of C–S–H, reflects this difference. The greater weight loss in this range for the 20 °C sample suggests the formation of a larger quantity of C–S–H, the primary hydration product [20, 40]. These findings demonstrate that, although daily thermal cycles enhance hydration in the early stages, they appear to inhibit continued hydration at later stages compared to constant curing at 20 °C. This phenomenon is also referred as "crossover effect" which is mentioned in the introduction. In the early stage of cement hydration, high curing temperatures promote the hydration reaction, leading to the rapid formation of hydration products. Due to the low solubility and diffusivity of the hydration products, they cannot effectively spread in the time allowed by rapid hydration. As a result, the rapidly formed hydration products precipitate quickly on the anhydrous cement particles, forming a dense layer. This layer slows down or even obstructs further hydration, ultimately leading to a lower degree of hydration of the anhydrous cement [14, 18, 20, 40, 55].

The MIP results presented in Figs. 9 and 10 illustrate the evolution of pore structure in samples containing 20% cement, cured under different thermal conditions for 3 and 28 days, respectively. Figures 9(a) and 10(a) present the cumulative pore volume per gram of sample, while Figs. 9(b) and 10(b) show the pore size distribution. After 3 days of curing, as shown in Fig. 9(a), the sample of SMC20%-Daily Thermal Cycle shows a lower cumulative pore volume of 0.2675 ml/g compared to 0.2849 ml/g for the sample cured at 20 °C. This reduction in total pore volume indicates early-stage densification under daily thermal cycles, which contributes directly to the enhanced strength and modulus observed in the mechanical tests. The pore size distribution in Fig. 9(b) further demonstrates that samples cured under daily thermal cycles exhibit a smaller proportion of medium-sized pores (10–0.05 μm), indicating pore refinement and a finer microstructure compared to samples cured at 20 °C. The MIP test results of the 28-day samples reveal a similar trend. In Fig. 10(a), the cumulative pore volume of the sample cured

under daily thermal cycles is 0.2248 ml/g, lower than the 0.2312 ml/g observed for the 20 °C cured sample. This continued reduction in porosity confirms that daily thermal cycles promote sustained microstructural densification. The pore size distribution in Fig. 10(b) shows that samples cured at 20 °C contain a greater proportion of medium-sized pores, resulting in a relatively coarser structure, whereas daily thermal cycling leads to a finer pore network.

At both early and late stages of curing, the samples subjected to daily thermal cycles exhibit lower porosity, a finer pore structure, and a reduced proportion of medium-sized pores. These microstructural refinements enhance load transfer within the cement-treated matrix and are consistent with the higher UCS and stiffness values measured in the strength tests. However, the "crossover effect" observed in the TG/DTG test results is not reflected in the MIP test results. This discrepancy may be attributed to the high water content in sensitive marine clay, which leads to an elevated water-to-cement (w/c) ratio in cement-stabilized SMC, resulting in a "dilution effect". Unlike traditional concrete—where the w/c ratio typically ranges between 0.4 and 0.6—the cement-stabilized SMC incorporates significantly more water. As a result, cement particles are surrounded by a larger volume of water, facilitating the long-distance diffusion of hydration products. This diffusion reduces the likelihood of hydration products precipitating directly around unhydrated cement particles [18], potentially altering the microstructural evolution. The absence of the crossover effect in the pore structure, as indicated by the MIP results, represents another noteworthy finding of this study.

Overall, the TG/DTG results confirm that daily thermal cycles accelerated early hydration (greater early-stage dehydration-related mass loss), while the MIP results show persistent pore refinement and reduced cumulative pore volume under thermal cycling. These microstructural changes provide a mechanistic basis for the higher early-age UCS and secant modulus (Sect. "Effect of Daily Thermal Cycles on Strength and Modulus-Development ") and the higher early-age matric suction (Sect. "Effect of Daily Thermal Cycles on the Matric Suction"), since accelerated hydration increases water consumption [18] and refined pore networks intensify capillary effects [44]. Together, the coupled hydration–pore refinement–suction evolution explains why daily thermal cycling produced faster early-age strengthening and stiffening, while the later-age hydration trend reflected the crossover effect discussed in the TG/DTG analysis [14, 40, 55].

Summary and conclusion

This study examined the effects of realistic summer daily thermal cycles on the mechanical, hydraulic, and microstructural behavior of cement-stabilized sensitive marine clay (SMC), a problematic subgrade material common in Eastern Canada. Laboratory experiments were conducted on samples stabilized with 5% and 20% cement and subjected to either constant curing at 20 °C or daily thermal cycles over a 28-day period. The evolution of strength, stiffness, matric suction, and microstructure was examined using unconfined compressive strength (UCS), secant modulus tests, matric suction monitoring, thermogravimetric analysis (TG/DTG), and mercury intrusion porosimetry (MIP).

The key findings are as follows:

- Daily thermal cycles significantly accelerated the early-age strength and stiffness development of cement-stabilized SMC. Strength differences between thermal curing regimes were most pronounced during the first week of curing, with thermal

cycling enabling up to 265% higher UCS at day 1 compared to constant-temperature curing. However, this early advantage diminished over time, leading to comparable or slightly lower strength values at later stages due to reduced hydration rates—a phenomenon consistent with the "crossover effect."

- TG/DTG analyses confirmed that thermal cycling promotes greater early-stage formation of hydration products such as C–S–H and ettringite. However, after 28 days, samples cured at 20 °C exhibited higher overall hydration levels, confirming the delayed strength gain associated with steady curing. Interestingly, MIP results showed that thermal cycling consistently produced denser microstructures with lower porosity and finer pore size distribution at both early and late curing stages, indicating complex interactions between thermal curing, hydration kinetics, and microstructural refinement.
- Thermal cycling significantly increased matric suction during early curing due to accelerated self-desiccation driven by faster hydration. Suction differences between the two curing conditions narrowed over time, indicating a deceleration of hydration under thermal cycling at later stages.

Overall, the findings demonstrate that summer daily thermal cycles play a dual role in the performance of cement-stabilized SMC: they enhance early strength and stiffness development, which can be beneficial for accelerating subgrade readiness and reducing construction delays, but may limit long-term hydration and strength gain due to the formation of hydration product layers that hinder further cement reaction. These results offer valuable insights for optimizing curing strategies and binder dosages in road and infrastructure projects involving sensitive marine clays under fluctuating thermal conditions. However, this study is limited to laboratory-scale specimens, a single cement type, and simulated summer thermal cycles over a 28-day curing period, which may not fully capture longer-term behavior, seasonal variability, and field-scale boundary conditions. Future work should include field validation, extended curing durations, and the use of alternative or blended binders to assess long-term durability and to mitigate the late-age hydration limitations observed under thermal cycling.

Author contributions
Zhe Liu: Investigation, Visualization, Writing - original draft. Mamadou Fall: Conceptualization, Methodology, Supervision, Writing - review & editing, Resources, Project administration, Funding acquisition.

Funding
This work was supported by the Natural Sciences and Engineering Research Council of Canada (NSERC) and the University of Ottawa.

Data availability
No datasets were generated or analysed during the current study.

Declarations

Competing interests
The authors declare no competing interests.

Received: 30 June 2025 / Accepted: 13 April 2026
Published online: 01 June 2026

References

1. Al-Moselly Z, Fall M (2024) Sulphate influence on strength development of cemented paste backfill with superplasticizer under field-like curing conditions. Constr Build Mater 451:138788. https://doi.org/10.1016/j.conbuildmat.2024.138788

2. Al-Umar M, Fall M, Daneshfar B (2020) GIS-based modeling of snowmelt-induced landslide susceptibility of sensitive marine clays. Geoenvironmental Disasters 7:9. https://doi.org/10.1186/s40677-020-0142-8
3. An Y, Zhang G (2024) Testing and prediction of mechanical characteristics of sensitive marine clays stabilized by deep mixing method. Mar Georesources Geotechnology 1–16. https://doi.org/10.1080/1064119X.2024.2392276
4. Aytekin M (1998) Soil stabilization with lime and cement. Digets December 1998, 471–477
5. Bayatvarkeshi M, Bhagat SK, Mohammadi K, Kisi O, Farahani M, Hasani A, Deo R, Yaseen ZM (2021) Modeling soil temperature using air temperature features in diverse climatic conditions with complementary machine learning models. Comput Electron Agric 185:106158. https://doi.org/10.1016/j.compag.2021.106158
6. Benkirane O, Haruna S, Fall M (2023) Strength and microstructure of cemented paste backfill modified with nano-silica particles and cured under non-isothermal conditions. Powder Technol 419:118311. https://doi.org/10.1016/j.powtec.2023.118311
7. Benson DO, Dirmeyer PA (2021) Characterizing the Relationship between Temperature and Soil Moisture Extremes and Their Role in the Exacerbation of Heat Waves over the Contiguous United States. J Clim 34:2175–2187. https://doi.org/10.1175/JCLI-D-20-0440.1
8. Bentley SP, Smalley IJ (1979) Mineralogy of a leda/champlain clay from gloucester (Ottawa, Ontario). Eng Geol 14:209–217. https://doi.org/10.1016/0013-7952(79)90086-3
9. Boardman DI, Glendinning S, Rogers CDF (2001) Development of stabilisation and solidification in lime–clay mixes. Géotechnique 51(6):533–543
10. Boquera L, Castro JR, Pisello AL, Fabiani C, D'Alessandro A, Ubertini F, Cabeza LF (2022) Effect of the curing process on the thermomechanical properties of calcium aluminate cement paste under thermal cycling at high temperatures for thermal energy storage applications. J Energy Storage 56:106039. https://doi.org/10.1016/j.est.2022.106039
11. Brooks GR (2014) Prehistoric Sensitive Clay Landslides and Paleoseismicity in the Ottawa Valley, Canada. In: L'Heureux J-S, Locat A, Leroueil S, Demers D, Locat J (eds) Landslides in Sensitive Clays: From Geosciences to Risk Management. Springer Netherlands, Dordrecht, pp 119–131. https://doi.org/10.1007/978-94-007-7079-9_10
12. Bruce MEC, Berg RR, Filz GM, Terashi M, Yang DS, Collin JG (2013) Federal Highway Administration Design Manual. Deep Mixing for Embankment and Foundation Support
13. Cao Y, Detwiler RJ (1995) Backscattered electron imaging of cement pastes cured at elevated temperatures. Cem Concr Res 25:627–638. https://doi.org/10.1016/0008-8846(95)00051-D
14. Chitambira B, Al-Tabbaa A, Perera A, Yu X (2007) The activation energy of stabilised/solidified contaminated soils. J Hazard Mater 141:422–429
15. Daily Data | Canada's National Climate Archive (2012) archive.ph. Available at: https://archive.ph/vteE
16. Eden WJ, Crawford CB (1957) Geotechnical properties of Leda clay in the Ottawa area / Les propriétés géotechniques de l'argile Leda dans la région d'Ottawa, in: Proceedings of the Fourth International Conference on Soil Mechanics and Foundation Engineering. Presented at the The Fourth International Conference on Soil Mechanics and Foundation Engineering, BUILDING RESEARCH, London, pp. 22–27
17. Elkhadiri I, Palacios M, Puertas F (2009) Effect of Curing Temperature on Cement Hydration. Ceram-Silik 53:65–75
18. Fall M, Célestin JC, Pokharel M, Touré M (2010) A contribution to understanding the effects of curing temperature on the mechanical properties of mine cemented tailings backfill. Eng Geol 114:397–413. https://doi.org/10.1016/j.enggeo.2010.05.016
19. Fang K, Fall M (2019) Chemically Induced Changes in the Shear Behaviour of Interface Between Rock and Tailings Backfill Undergoing Cementation. Rock Mech Rock Eng 52:3047–3062. https://doi.org/10.1007/s00603-019-01757-0
20. Fang K, Fall M (2018) Effects of curing temperature on shear behaviour of cemented paste backfill-rock interface. Int J Rock Mech Min Sci 112:184–192. https://doi.org/10.1016/j.ijrmms.2018.10.024
21. Government of Canada (2024) Daily Maximum Temperature for August 1936. Available at: https://climate.weather.gc.ca
22. Gulec A (2023) Investigation of the effect of different curing conditions on the mechanical performance of calcium aluminate cement concrete at elevated temperatures. Constr Build Mater 409:133920. https://doi.org/10.1016/j.conbuildmat.2023.133920
23. Hannant DJ (2000) 4.11 - Cement-based Composites. In: Kelly A, Zweben C (eds) Comprehensive Composite Materials. Pergamon, Oxford, pp 323–362. https://doi.org/10.1016/B0-08-042993-9/00098-X
24. Heidarabadizadeh N, Ghanizadeh AR, Behnood A (2021) Prediction of the resilient modulus of non-cohesive subgrade soils and unbound subbase materials using a hybrid support vector machine method and colliding bodies optimization algorithm. Constr Build Mater 275:122140. https://doi.org/10.1016/j.conbuildmat.2020.122140
25. Ho LS, Nakarai K, Eguchi K, Sasaki T, Morioka M (2018) Strength development of cement-treated sand using different cement types cured at different temperatures. MATEC Web Conf 195. https://doi.org/10.1051/matecconf/201819501006
26. Jennings HM, Thomas J, Rothstein D, Chen J (2002) Cements as porous materials. Handb porous solids 2971–3028
27. Khemissa M, Mahamedi A (2014) Cement and lime mixture stabilization of an expansive overconsolidated clay. Appl Clay Sci 95:104–110
28. Kim JK, Moon YH, Eo SH (1998) Compressive strength development of concrete with different curing time and temperature. Cem Concr Res 28:1761–1773. https://doi.org/10.1016/S0008-8846(98)00164-1
29. Kojima K, Kim J, Kitagaki R, Hama Y (2023) Study of microstructural changes in blast-furnace cement hardened by repeated dry and wet curing at high temperatures. Constr Build Mater 403:132861. https://doi.org/10.1016/j.conbuildmat.2023.132861
30. Kjellsen KO, Detwiler RJ (1992) Reaction kinetics of portland cement mortars hydrated at different temperatures. Cem Concr Res 22:112–120. https://doi.org/10.1016/0008-8846(92)90141-H
31. Lerch W, Bogue RH (1934) The heat of hydration of portland cement pastes. Portland Cement Association at the National Bureau of Standards Washington …
32. Li L, Fall M (2019) Shear behaviour of Canadian marine clay/geomembrane interface under freeze–thaw cycles. Environ Geotechnics 8(4):246–254
33. Li S, Kirstein A, Gurpersaud N, Liu J (2016) Experimental investigation of cement mixing to improve Champlain Sea clay

34. Li W, Liu AS, Kwok CY, Sit CY, Shiu HK (2023) Mechanical behaviour of Hong Kong marine deposits stabilized with high content of coal fly ash. Constr Build Mater 392:131837. https://doi.org/10.1016/j.conbuildmat.2023.131837
35. Liu S, Fall M (2024) The significance of mixing time in the development of the engineering properties of cemented fiber-reinforced tailings materials. J Building Eng 96:110648. https://doi.org/10.1016/j.jobe.2024.110648
36. Lu J, Liu J, Yang H, Gao J, Wan X, Zhang J (2022) Influence of curing temperatures on the performances of fiber-reinforced concrete. Constr Build Mater 339:127640. https://doi.org/10.1016/j.conbuildmat.2022.127640
37. Lu J, Tan L, Pei W, Gao J, Deng F, Zhou X, Zhang Z (2024) Shear behavior of cement-stabilized silty clay exposed to low-temperature curing. Cold Reg Sci Technol 223:104215. https://doi.org/10.1016/j.coldregions.2024.104215
38. Marchon D, Flatt RJ (2016) 8 - Mechanisms of cement hydration, in: Aïtcin, P.-C., Flatt, Robert J (Eds.), Science and Technology of Concrete Admixtures. Woodhead Publishing, pp. 129–145. https://doi.org/10.1016/B978-0-08-100693-1.00008-4
39. Marzano I, Al-Tabbaa A, Grisolia M (2008) Influence of curing temperature on the strength of cement-stabilised artificial clays. Presented at the Proc., 2nd Int. Workshop on Geotechnics of Soft Soils, pp. 257–262
40. Mindess S (2019) Developments in the Formulation and Reinforcement of Concrete. Woodhead Publishing
41. Moir G (2003) 1 - Cements. In: Newman J, Choo BS (eds) Advanced Concrete Technology. Butterworth-Heinemann, Oxford, pp 3–45. https://doi.org/10.1016/B978-075065686-3/50277-9.
42. Nader A, Fall M, Hache R (2015) Characterization of Sensitive Marine Clays by Using Cone and Ball Penetrometers: Example of Clays in Eastern Canada. Geotech Geol Eng 33, 841–864 (2015). https://doi.org/10.1007/s10706-015-9864-x
43. Nader A (2014) Engineering Characteristics of Sensitive Marine Clays - Examples of Clays in Eastern Canada (Article). University of Ottawa, Ottawa, Ontario, Canada
44. Pham TA, Hashemi A, Sutman M, Medero GM (2023) Effect of temperature on the soil–water retention characteristics in unsaturated soils: Analytical and experimental approaches. Soils Found 63:101301. https://doi.org/10.1016/j.sandf.2023.101301
45. Pichler C, Schmid M, Traxl R, Lackner R (2017) Influence of curing temperature dependent microstructure on early-age concrete strength development. Cem Concr Res 102:48–59. https://doi.org/10.1016/j.cemconres.2017.08.022
46. Quan W, Fall M (2024) Temperature-driven crack self-healing and performance recovery in cemented tailings materials. Case Stud Constr Mater 21:e04105. https://doi.org/10.1016/j.cscm.2024.e04105
47. Quigley RM (1980) Geology, mineralogy, and geochemistry of Canadian soft soils: a geotechnical perspective. Can Geotech J 17:261–285
48. Rajasekaran G, Narasimha Rao S (2002) Permeability characteristics of lime treated marine clay. Ocean Eng 29:113–127. https://doi.org/10.1016/S0029-8018(01)00017-8
49. Roshan MJ, Rashid A, Abdul Wahab AS, Tamassoki N, Jusoh S, Hezmi SN, Nik Daud MA, Apandi NNM, Azmi N, M (2022) Improved methods to prevent railway embankment failure and subgrade degradation: A review. Transp Geotechnics 37:100834. https://doi.org/10.1016/j.trgeo.2022.100834
50. Sagade A, Fall M, Al-Moselly Z (2023) Strength and suction development of cemented paste backfill with ternary cement blends. Can J Civ Eng 51:11–26. https://doi.org/10.1139/cjce-2023-0020
51. Saremi A, Fall M (2024) Self-desiccation behavior of nano-cemented tailings backfill plug: Insights from thermo-mechanical-chemical column experiments. J Mater Res Technol 30:5952–5962. https://doi.org/10.1016/j.jmrt.2024.04.189
52. Sasanian S (2011) The Behaviour of Cement Stabilized Clay At High Water Contents (Article). University of Western Ontario, London, Ontario, Canada
53. Sharma P, Shukla M, Sammis T (2010) Predicting Soil Temperature Using Air Temperature and Soil, Crop, and Meteorological Parameters for Three Specialty Crops in Southern New Mexico. Appl Eng Agric 26:47–58. https://doi.org/10.13031/2013.29474
54. Song MM, Feng J, Zhong XG, Wu H, Yao D (2022) Strength Properties of Cement-Treated Lean Clay Cured at Constant and Changing Temperature. J Mater Civ Eng 34:04022233. https://doi.org/10.1061/(ASCE)MT.1943-5533.0004387
55. Soroka I (1993) Concrete in hot environments. CRC
56. Taha A, Fall M (2014) Shear behavior of sensitive marine clay–steel interfaces. Acta Geotech 9:969–980. https://doi.org/10.1007/s11440-014-0321-4
57. Taha A, Fall M (2013) Shear Behavior of Sensitive Marine Clay-Concrete Interfaces. J Geotech GeoEnviron Eng 139:644–650. https://doi.org/10.1061/(ASCE)GT.1943-5606.0000795
58. Termkhajornkit P, Barbarulo R (2012) Modeling the coupled effects of temperature and fineness of Portland cement on the hydration kinetics in cement paste. Cem Concr Res 42:526–538. https://doi.org/10.1016/j.cemconres.2011.11.016
59. Thomas JJ, Jennings HM (2006) A colloidal interpretation of chemical aging of the C-S-H gel and its effects on the properties of cement paste. Cem Concr Res 36:30–38. https://doi.org/10.1016/j.cemconres.2004.10.022
60. Tian X, Fall M (2021) Non-isothermal evolution of mechanical properties, pore structure and self-desiccation of cemented paste backfill. Constr Build Mater 297:123657. https://doi.org/10.1016/j.conbuildmat.2021.123657
61. Tunono C, Fall M (2024a) Column experiments to study the thermo-hydro-mechanical-chemical behavior of sensitive marine slay subgrade soil treated with lime. Bull Eng Geol Environ 83, 120 (2024). https://doi.org/10.1007/s10064-024-03637-6
62. Tunono C, Fall M (2024b) THMC Behavior of Lime-Stabilized Clay Subgrade Under Daily Thermal Cycles: Column Experiments. Geotech Geol Eng 42:915–944. https://doi.org/10.1007/s10706-023-02596-1
63. Wang Y, Fall M, Wu A (2016) Initial temperature-dependence of strength development and self-desiccation in cemented paste backfill that contains sodium silicate. Cem Concr Compos 67:101–110. https://doi.org/10.1016/j.cemconcomp.2016.01.005
64. Xu F, Lin X, Zhou A (2023) Microstructure change and mechanical property variation of high performance concrete with recycled ceramic aggregate as internal curing material under different environmental temperatures. Constr Build Mater 369:130636. https://doi.org/10.1016/j.conbuildmat.2023.130636

65. Yin D, Wang L, Wang Z, Yin L, Liu S, Li L (2024) Enhancing shear resistance in pavement structures with crumb rubber modified asphalt gravel as a bonding layer. Constr Build Mater 426:136184. https://doi.org/10.1016/j.conbuildmat.2024.136184
66. Zhang RJ, Lu YT, Tan TS, Phoon KK, Santoso AM (2014) Long-Term Effect of Curing Temperature on the Strength Behavior of Cement-Stabilized Clay. J Geotech GeoEnviron Eng 140:04014045. https://doi.org/10.1061/(ASCE)GT.1943-5606.0001144
67. Zimar Z, Robert D, Zhou A, Giustozzi F, Setunge S, Kodikara J (2022) Application of coal fly ash in pavement subgrade stabilisation: A review. J Environ Manage 312:114926. https://doi.org/10.1016/j.jenvman.2022.114926

Publisher's Note